Effect of Atmospheric Turbulence on BER Performance of FSO System Based on Various Modulation Techniques

Mini Sengar, Devendra Soni

***Abstract*— In this paper we have analyzed performance of free space optical (FSO) communication system in terms of BER (Bit Error Rate) based on various modulation schemes under the influence of different atmospheric turbulence conditions. This analysis is performed in light fog (attenuation is 4.285 dB/Km) condition. Modulation schemes utilized are OOK (On-off keying), BPSK (Binary phase shift keying), 16-PSK, 2-PPM (Pulse phase modulation), 16- PPM, 4-QAM, 16-QAM, DPSK (phase shift keying), 8-PAM (Pulse amplitude modulation) and 16-PAM. This analysis is performed in MATLAB tool. BER versus SNR graph is generated for all modulation techniques. Simulation is performed at 1550 nm wavelength. Atmospheric turbulence is weak turbulence (C_n^2=8.4 x 10^{-15} $m^{-2/3}$), moderate turbulence (C^2=1.7 x 10^{-14} $m^{-2/3}$) and strong turbulence (C^2=5 x 10^{-14} $m^{-2/3}$)**

***Index Terms*— Atmospheric Turbulence, PSK, Light Fog, BER, SNR.**

I. INTRODUCTION

With rapid development and maturity in the optoelectronic devices, FSO has now witnessed a restore in many applications. Recently, radio-on-free-space optics (RoFSO) technology is regarded as a new universal platform for enabling seamless convergence of fiber and FSO communication networks, thus extending broadband connectivity to underserved areas. In an alternative internet access method is proposed using WLAN and FSO systems as a data uplink and digital video broadcasting – terrestrial (DVB-T) as a downlink channel for broadband data access network. Several successful field trials have been recorded in the last few years including the 147 km FSO transmission which have further encouraged investments in the field. This has now culminated into the increased commercialisation and the deployment of FSO in today's communication infrastructures.

FSO link performance is degraded by the substantial optical signal losses due to the presence of aerosols by absorption and scattering of the propagating optical and infrared waves, since their wavelengths are very close to the wavelengths of these frequencies. Fog compared to other atmospheric constituents is the dominant source for the optical power attenuation, thus potentially reducing the FSO link availability. However, in the clear weather condition, theoretical and experimental studies have shown that scintillation can severely degrade the reliability and connectivity of FSO links. Nevertheless, the atmospheric channel effects such as thick fog, smoke and turbulence poses a great challenge to achieve the link availability and reliability according to the IEEE and ITU link availability standards of 99.999% (five nines) for the last mile access communication network.

When turbulence effects are included, the effects of the atmosphere are in a sense subtler. This optical turbulence is caused almost exclusively by temperature variations in the atmosphere, resulting in random variations of refractive index. An optical wave propagating through the atmospheric turbulence will experience random amplitude and phase fluctuations, which will generate a number of effects: break-up of the beam into distinct patches of fluctuating illumination, wander of the centroid of the beam, and increase in the beam width over the expected diffraction limit. For longer links, the problems presented by atmospheric turbulence are quite severe, since the average power received at the FSO receiver will decrease even more.

II. ATMOSPHERIC TURBULENCE

Refractive index fluctuations of the atmosphere are an important parameter in optical wave propagation. These fluctuations are triggered by the change in the wind velocity *v*w and temperature *Te* of the atmosphere. A combination of small changes in *v*w and *Te* induces a random behaviour in the atmospheric refractive index. the dependency of the wavelength on the refractive index fluctuations is significantly small and can therefore be ignored for optical frequencies. The contribution of humidity in refractive index fluctuation is insignificant in the FIR region and pressure fluctuations are also usually negligible. Therefore, the refractive index fluctuations in the range of visible and NIR regions are mostly dependent on the random temperature fluctuations.

The turbulence over the free space channel is modeled as gamma-gamma distribution in induced fading channel. The channel of FSO communication link is modeled by considering the atmospheric attenuation with channel loss (hp), due to different fog strength (light fog and moderate fog) and the scintillation (hs) due to atmospheric turbulence. The relation between the channel loss and scintillation is given as h = hp.hs

Atmospheric turbulence due to fluctuation in air mass is modeled by gamma-gamma distributed channel and expressed as,

$$f_{h_s}(h_s) = \frac{2\left(\alpha\beta^{(\alpha+\beta)/2}\right)}{\Gamma(\alpha)\Gamma(\beta)} h_s^{\frac{\alpha+\beta}{2}-1} K_{\alpha-\beta}(2\sqrt{\alpha\beta h_s})$$

Mini Sengar, P. G. Scholar (Electronics & Comm.), Arya Institute of Engineering & Technology, Jaipur
Devendra Soni, Assistant Professor (Electronics & Comm.), Arya Institute of Engineering & Technology, Jaipur

where, α and β are the values of spherical wave, the distribution shaping parameter, Kα-β (.) represents the modified second order Bessel function, Γ(.) denotes the gamma function. α and β can be defined as,

$$\alpha = \left(exp\left[\frac{0.49 D_0^2}{\left(1 + 0.56 D_0^{12/5}\right)^{7/6}} \right] - 1 \right)^{-1}$$

$$\beta = \left(exp\left[\frac{0.51 D_0^2}{\left(1 + 0.69 D_0^{12/5}\right)^{5/6}} \right] - 1 \right)^{-1}$$

where, $D_0^2 = 0.5 C_n^2 k^{7/6} z^{11/6}$, represents the Rytov variance of spherical wave, C_n^2 is the refractive index or strength of turbulence, k = 2π / λ, is the optical wave number, and λ is the operating wavelength.

Probability density function (pdf) of the channel ($f_h(h)$) can be represented as follows.

$$f_h(h) = \left| \frac{d}{dh}\left(\frac{h}{h_p}\right) \right| f_{h_s}\left(\frac{h}{h_p}\right)$$

The above Bessel function can be formulated in terms of Meijer-G function [60] as follows.

$$K_v(z) = \frac{1}{2} G_{0,2}^{2,0}\left[\frac{z^2}{4} \middle| \begin{matrix} - \\ \frac{v}{2}, \frac{-v}{2} \end{matrix} \right]$$

Gamma-gamma distributed channel can be expressed using Meijer-G as follows.

$$f_{h_s}(h_s) = \frac{\left(\alpha\beta^{(\alpha+\beta)/2}\right)}{\Gamma(\alpha)\Gamma(\beta)} h_s^{\frac{\alpha+\beta}{2}-1} G_{0,2}^{2,0}\left[\alpha\beta h_s \middle| \begin{matrix} \frac{\alpha-\beta}{2}, \frac{\beta-\alpha}{2} \end{matrix} \right]$$

Now, the probability density function of the atmospheric turbulence channel is given

$$f_h(h) = \frac{\left(\alpha\beta^{(\alpha+\beta)/2}\right)}{\Gamma(\alpha)\Gamma(\beta)} \frac{h^{\frac{\alpha+\beta}{2}-1}}{h_p^{\frac{\alpha+\beta}{2}-1}} G_{0,2}^{2,0}\left[\alpha\beta \frac{h}{h_p} \middle| \begin{matrix} \frac{\alpha-\beta}{2}, \frac{\beta-\alpha}{2} \end{matrix} \right]$$

As the turbulence increases from a weak to a strong regime, the distribution spreads out more, with an increase in the range of possible values of the scintillation.

III. BER FOR VARIOUS MODULATION TECHNIQUES

a. OOK (ON-OFF KEYING)

The Pe(h) for ON-OFF keying can be expressed using Meijer-G as follows:

$$P_e(h) = \frac{1}{2\sqrt{\pi}} G_{1,2}^{2,0}\left[\frac{\gamma h^2}{2} \middle| \begin{matrix} 1 \\ 0, \frac{1}{2} \end{matrix} \right]$$

BER expression can be written as:

$$BER = Q_0 G_{5,2}^{2,4}\left[\frac{8\gamma {h_p}^2}{(\alpha\beta)^2} \middle| \begin{matrix} \frac{1-\alpha}{2}, 1-\frac{\alpha}{2}, \frac{1-\beta}{2}, 1-\frac{\beta}{2}, 1 \\ 0, \frac{1}{2} \end{matrix} \right]$$

Where γh2 denotes instantaneous value of SNR, γ denotes mean electrical output value of SNR and Q0 = 2α+β/8π3/2 Γ(α) Γ(β)

b. *BPSK (Binary Shift Keying)*

The Pe(h) for BPSK can be expressed using Meijer-G as follows:

$$P_e(h) = \frac{1}{2\sqrt{\pi}} G_{1,2}^{2,0}\left[\gamma h^2 \middle| \begin{matrix} 1 \\ 0, \frac{1}{2} \end{matrix} \right]$$

BER expression can be written as:

$$BER = Q_0 G_{5,2}^{2,4}\left[\frac{16\gamma {h_p}^2}{(\alpha\beta)^2} \middle| \begin{matrix} \frac{1-\alpha}{2}, 1-\frac{\alpha}{2}, \frac{1-\beta}{2}, 1-\frac{\beta}{2}, 1 \\ 0, \frac{1}{2} \end{matrix} \right]$$

Where Q0 = 2α+β/8π3/2 Γ(α) Γ(β)

c. *16-PSK (Phase Shift Keying)*

The Pe(h) for 16-PSK keying can be expressed using Meijer-G as follows:

$$P_e(h) = \frac{1}{4\sqrt{\pi}} G_{1,2}^{2,0}\left[\frac{8\gamma h^2}{50} \middle| \begin{matrix} 1 \\ 0, \frac{1}{2} \end{matrix} \right]$$

BER expression can be written as:

$$BER = \frac{Q_0}{2} G_{5,2}^{2,4}\left[\frac{64\gamma {h_p}^2}{25(\alpha\beta)^2} \middle| \begin{matrix} \frac{1-\alpha}{2}, 1-\frac{\alpha}{2}, \frac{1-\beta}{2}, 1-\frac{\beta}{2}, 1 \\ 0, \frac{1}{2} \end{matrix} \right]$$

Where Q0 = 2α+β/8π3/2 Γ(α) Γ(β)

d. *2-PPM (Pulse Phase Modulation)*

The Pe(h) for 2-PPM can be expressed using Meijer-G as follows:

$$P_e(h) = \frac{1}{2\sqrt{\pi}} G_{1,2}^{2,0}\left[\frac{\gamma h^2}{8} \middle| \begin{matrix} 1 \\ 0, \frac{1}{2} \end{matrix} \right]$$

BER expression can be written as:

$$BER = Q_0 G_{5,2}^{2,4}\left[\frac{2\gamma {h_p}^2}{(\alpha\beta)^2} \middle| \begin{matrix} \frac{1-\alpha}{2}, 1-\frac{\alpha}{2}, \frac{1-\beta}{2}, 1-\frac{\beta}{2}, 1 \\ 0, \frac{1}{2} \end{matrix} \right]$$

Where Q0 = 2α+β/8π3/2 Γ(α) Γ(β)

e. *16-PPM (Pulse Phase Modulation)*

The Pe(h) for 16-PPM can be expressed using Meijer-G as follows:

$$P_e(h) = \frac{1}{2\sqrt{\pi}} G_{1,2}^{2,0}\left[4\gamma h^2 \middle| \begin{matrix} 1 \\ 0, \frac{1}{2} \end{matrix}\right]$$

BER expression can be written as:

$$BER = Q_0 G_{5,2}^{2,4}\left[\frac{64\gamma h_p^{\,2}}{(\alpha\beta)^2}\middle| \begin{matrix} \frac{1-\alpha}{2}, 1-\frac{\alpha}{2}, \frac{1-\beta}{2}, 1-\frac{\beta}{2}, 1 \\ 0, \frac{1}{2} \end{matrix}\right]$$

Where Q0 = $2^{\alpha+\beta}/8\pi^{3/2}$ Γ(α) Γ(β)

f. 4-QAM (Quadrature Amplitude Modulation)

The Pe(h) for 4-QAM can be expressed using Meijer-G as follows:

$$P_e(h) = \frac{3}{2\sqrt{\pi}} G_{1,2}^{2,0}\left[\gamma h^2 \middle| \begin{matrix} 1 \\ 0, \frac{1}{2} \end{matrix}\right]$$

BER expression can be written as:

$$BER = 3\, Q_0 G_{5,2}^{2,4}\left[\frac{16\gamma h_p^{\,2}}{(\alpha\beta)^2}\middle| \begin{matrix} \frac{1-\alpha}{2}, 1-\frac{\alpha}{2}, \frac{1-\beta}{2}, 1-\frac{\beta}{2}, 1 \\ 0, \frac{1}{2} \end{matrix}\right]$$

Where Q0 = $2^{\alpha+\beta}/8\pi^{3/2}$ Γ(α) Γ(β)

g. 16-QAM (Quadrature Amplitude Modulation)

The Pe(h) for 16-QAM can be expressed using Meijer-G as follows:

$$P_e(h) = \frac{15}{8\sqrt{\pi}} G_{1,2}^{2,0}\left[\gamma h^2 \middle| \begin{matrix} 1 \\ 0, \frac{1}{2} \end{matrix}\right]$$

BER expression can be written as:

$$BER = \frac{15\, Q_0}{4} G_{5,2}^{2,4}\left[\frac{16\gamma h_p^{\,2}}{(\alpha\beta)^2}\middle| \begin{matrix} \frac{1-\alpha}{2}, 1-\frac{\alpha}{2}, \frac{1-\beta}{2}, 1-\frac{\beta}{2}, 1 \\ 0, \frac{1}{2} \end{matrix}\right]$$

Where Q0 = $2^{\alpha+\beta}/8\pi^{3/2}$ Γ(α) Γ(β)

h. DPSK (Differential Phase Shift Keying)

The Pe(h) for DPSK can be expressed using Meijer-G as follows:

$$P_e(h) = \frac{1}{2\sqrt{\pi}} G_{1,2}^{2,0}\left[\frac{\gamma h^2}{8}\middle| \begin{matrix} 1 \\ 0, \frac{1}{2} \end{matrix}\right]$$

BER expression can be written as:

$$BER = Q_0 G_{5,2}^{2,4}\left[\frac{2\gamma h_p^{\,2}}{(\alpha\beta)^2}\middle| \begin{matrix} \frac{1-\alpha}{2}, 1-\frac{\alpha}{2}, \frac{1-\beta}{2}, 1-\frac{\beta}{2}, 1 \\ 0, \frac{1}{2} \end{matrix}\right]$$

Where Q0 = $2^{\alpha+\beta}/8\pi^{3/2}$ Γ(α) Γ(β)

i. 8-PAM (Pulse Amplitude Modulation)

The Pe(h) for 8-PAM can be expressed using Meijer-G as follows:

$$P_e(h) = \frac{1}{2\sqrt{\pi}} G_{1,2}^{2,0}\left[\frac{3\gamma h^2}{224}\middle| \begin{matrix} 1 \\ 0, \frac{1}{2} \end{matrix}\right]$$

BER expression can be written as:

$$BER = Q_0 G_{5,2}^{2,4}\left[\frac{3\gamma h_p^{\,2}}{14(\alpha\beta)^2}\middle| \begin{matrix} \frac{1-\alpha}{2}, 1-\frac{\alpha}{2}, \frac{1-\beta}{2}, 1-\frac{\beta}{2}, 1 \\ 0, \frac{1}{2} \end{matrix}\right]$$

Where Q0 = 2α+β/8π3/2 Γ(α) Γ(β)

j. 16-PAM (Pulse Amplitude Modulation)

The Pe(h) for 16-PAM can be expressed using Meijer-G as follows:

$$P_e(h) = \frac{1}{2\sqrt{\pi}} G_{1,2}^{2,0}\left[\frac{\gamma h^2}{120}\middle| \begin{matrix} 1 \\ 0, \frac{1}{2} \end{matrix}\right]$$

BER expression can be written as:

$$BER = Q_0 G_{5,2}^{2,4}\left[\frac{2\gamma h_p^{\,2}}{15(\alpha\beta)^2}\middle| \begin{matrix} \frac{1-\alpha}{2}, 1-\frac{\alpha}{2}, \frac{1-\beta}{2}, 1-\frac{\beta}{2}, 1 \\ 0, \frac{1}{2} \end{matrix}\right]$$

Where Q0 = $2^{\alpha+\beta}/8\pi^{3/2}$ Γ(α) Γ(β)

IV. SIMULATION RESULTS

In this paper we have shown performance of FSO system based on various modulation techniques under the influence of atmospheric turbulence conditions such as *weak turbulence* (C_n^2=8.4 x 10^{-15} $m^{-2/3}$), *moderate turbulence* (C_n^2=1.7 x 10^{-14} $m^{-2/3}$) *and strong turbulence* (C_n^2=5 x 10^{-14} $m^{-2/3}$). All simulations have been performed in MATLAB simulation tool. BER versus SNR graph is generated to show the performance. All the simulations are performed in light fog condition. Fig. 1, 2 and 3 shows performance of FSO link under weak, moderate and strong turbulence respectively.

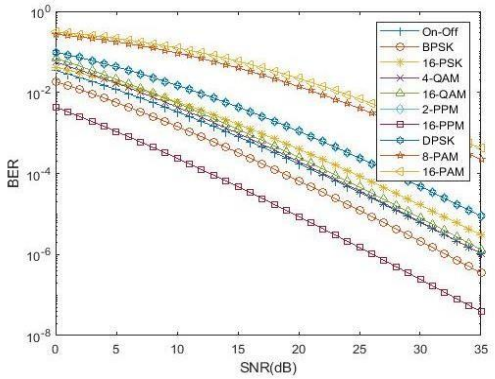

Fig 1 BER versus SNR for weak turbulence

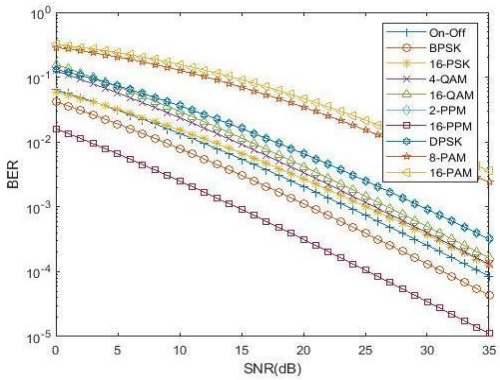

Fig 2 BER versus SNR for moderate turbulence

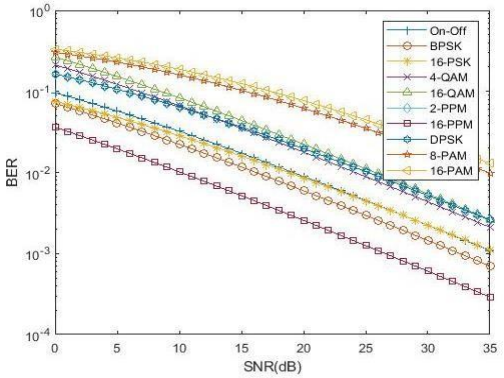

Fig 3 BER versus SNR for strong turbulence

V. CONCLUSIONS

In this work we have successfully analyzed BER performance of FSO system based on various modulation techniques under the influence of atmospheric turbulence conditions. It is observed that 16-PPM technique is showing better results among all techniques. As the atmospheric turbulence is increased, value of BER is also increased but still 16-PPM shows least BER value among all techniques.

REFERENCES

[1] A.C. Boucouvalas, .Challenges in Optical Wireless Communications., in Optics & Photonics News, Vol. 16, No. 5, 36-39 (2005).
[2] P. Gupta, P.R. Kumar, "The Capacity of Wireless Networks", IEEE, 2000.
[3] P. Mandl, P. Schrotter, and E. Leitgeb, "Hybrid systems using DVB-T, WLAN and FSO to connect peripheral regions with broadband Internet 220 services," in Telecommunications. ConTEL. 10th International Conference on, pp. 67-71, 2009.
[4] A. Pavelchek, R. Trissel, J. Plante, and S. Umbrasas, "Long wave infrared (10 micron) free space optical communication system," Proceedings of SPIE, 2004.
[5] J. C. Juarez, D. W. Young, J. E. Sluz, J. L. Riggins Ii, and D. H. Hughes, "Free-space optical channel propagation tests over a 147-km link,"Atmospheric Propagation VIII, pp. 80380B-80380B, 2011.
[6] G. Keiser, .Optical Fiber Communications., (McGraw-Hill, 2000).
[7] A. Soibel, M. W. Wright, W. H. Farr, S. A. Keo, C. J. Hill, R. Q. Yang, and H. C. Liu, "Midinfrared Interband Cascade Laser for Free Space Optical Communication," IEEE Photonics Technology Letters, vol. 22, pp. 121-123, 2009.
[8] W. Gappmair and M. Flohberger, "Error performance of coded FSO links in turbulent atmosphere modeled by gamma-gamma distributions," IEEE Transactions on Wireless Communications, vol. 8, pp. 2209-2213, 2009.
H. E. Nistazakis, T. A. Tsiftsis, and G. S. Tombras, "Performance analysis of free-space optical communication systems over atmospheric turbulence channels," Communications, IET, vol. 3, pp. 1402- 1409, 2009